(FOUO 6/80)

8 OCTOBER 1980

JPRS L/9335

8 October 1980

USSR Report

ENGINEERING AND EQUIPMENT

(FOUO 6/80)

FBIS FOREIGN BROADCAST INFORMATION SERVICE

NOTE

JPRS publications contain information primarily from foreign newspapers, periodicals and books, but also from news agency transmissions and broadcasts. Materials from foreign-language sources are translated; those from English-language sources are transcribed or reprinted, with the original phrasing and other characteristics retained.

Headlines, editorial reports, and material enclosed in brackets [] are supplied by JPRS. Processing indicators such as [Text] or [Excerpt] in the first line of each item, or following the last line of a brief, indicate how the original information was processed. Where no processing indicator is given, the information was summarized or extracted.

Unfamiliar names rendered phonetically or transliterated are enclosed in parentheses. Words or names preceded by a question mark and enclosed in parentheses were not clear in the original but have been supplied as appropriate in context. Other unattributed parenthetical notes within the body of an item originate with the source. Times within items are as given by source.

The contents of this publication in no way represent the policies, views or attitudes of the U.S. Government.

For further information on report content call (703) 351-2938 (economic); 3468 (political, sociological, military); 2726 (life sciences); 2725 (physical sciences).

APPROVED FOR RELEASE: 2007/02/08: CIA-RDP82-00850R000300040015-8

JPRS L/9335

8 October 1980

USSR REPORT

ENGINEERING AND EQUIPMENT

(FOUO 6/80)

CONTENTS

NON-NUCLEAR ENERGY

UDC 621.472:621.383.5(063)

THE DEVELOPMENT OF SOLAR BATTERIES FOR THE INTERPLANETARY AUTOMATIC STATIONS 'VENERA-9,' 'VENERA-10' AND FOR THE 'LUNOKHOD' PROGRAM

Tashkent GELIOTEKHNIKA in Russian No 4, Apr 80 pp 3-9

[Article by G. S. Daletskiy, M. B. Kagan, M. M. Koltun and V. M. Kuznetsov]

[Text] The utilization of solar batteries as the basic primary electric power-supply sources on space vehicles directed toward Venus or operating on the lunar surface possesses a number of specific features that preclude the application of silicon solar batteries of the usual design.

Chief among the operational peculiarities of solar batteries is the increase in the level of solar radiation reaching the battery along with the simultaneous rise in the operating temperature of the solar batteries (in the case of vehicles traveling to Venus) and the significant increase in the level of equilibrium operating temperatures of solar batteries exposed to constant solar radiation. This is in comparison with vehicles that operate in near-Earth space (as in the case of automatic self-propelled vehicles of the "Lunokhod" type, designed for extended operation on the lunar surface).

Calculations have shown that the equilibrium operating temperature is established at a level of 125-145°C for the solar batteries on the "Lunokhod" which are illuminated by the Sun and heated by the Moon's own considerable thermal radiation. For solar batteries composed of silicon solar cells of the usual design, a gradual increase in temperature from 65 to 150°C takes place along the flight path from Earth to Venus.

The application of passive temperature regulating methods for reducing the equilibrium operating temperature (for example, not tilting the panels directly at the Sun) or a basic decrease

in the panels' space factor in the aforementioned cases is not possible in view of the stringent demands on the dimensions and over-all design of the vehicles.

We have adopted the following as basic directions for the development of solar batteries in the given program: 1) the development of a model of a silicon solar cell which, for any level of solar radiation that reaches the cell, possesses a lowered equilibrium temperature in comparison with the usual design; 2) the creation of solar batteries with the help of a semiconducting material that has a broader forbidden band than silicon and which possesses an optimum combination of photoelectric and operational properties--gallium arsenide.

The Optical and Radiation Characteristics of Silicon Photoelectric Cells and of Solar Battery Models That Possess Reduced Equilibrium Temperatures. When operating under conditions of radiation heat exchange, the lower the equilibrium temperature of p-n junction semiconductor photoelectric transducers and the higher the electric output they produce, the lower the ratio of the integral coefficient of solar radiation absorption α_s to the integral coefficient of thermal radiation ε at the surface. When utilizing optical coatings--radiation-resistant glass [1] or transparent silicone lacquer [2]--the normal coefficient ε at the surface of the photoelectric transducer becomes equal to 0.9-0.92, instead of 0.2-0.25 in the absence of the coating, approaching its own limit of $\varepsilon_{\text{ABSOL. BLACK BODY}}=1.0$. The coefficient of radiation ε into the hemisphere is 0.84-0.86. The coefficient α_s for a photoelectric cell of the usual design is 0.92-0.93, which is considerably higher than its minimum value of 0.67, which can be achieved without reducing its efficiency.

Photoelectric cells of the usual design [3], as our measurements have shown, are opaque in the entire solar spectrum interval from 0.2 to 0.3 μm. This occurs because of radiation absorption by the free charge carriers in the comparatively thick, 2-3 μm, heavily doped surface layer of a photoelectric cell with a p-n junction, in the solid metallic backside element and at the semiconductor-metal interface.

The photoelectric transducer becomes transparent in the infrared region of the solar spectrum from 1.1 to 3.0 μm when a number of conditions are met [4]: the depth of the semiconductor's heavily doped upper layer is not to be more than 0.5-1.0 μm thick, the contact grid on the back side of the device is not to occupy more than 5-10 percent of the surface, the back side is to be highly polished and there is to be an effective reflection reducing coating on both surfaces of the device. With a transparent or wide-meshed supporting surface made from materials proposed, for example, in work [5], a solar battery made from

such photoelectric transducers possesses 80-90 percent less absorption in the region of the 1.1-3.0 μm spectrum than an ordinary battery. In this case, the coefficient α_s is equal to 0.7-0.72, while ε remains at a level of 0.9.

In place of white enamels that darken when exposed to the Sun's ultraviolet radiation, a stable selective coating has been developed. This coating possesses a low ratio of α_s/ε (less than 0.2) and is based upon glass films made from radiation-resistant glass with a vaporized aluminum or silver coating on the back surface [6]. This coating was utilized successfully to protect the cooling radiator on "Lunokhod" I and II from overheating.

In order to obtain such a low ratio of α_s/ε for photoelectric transducers that are occupied by the contacts, it was decided (in the design of parallel modules in which one piece of glass protects several large photoelectric transducers simultaneously) that the back surface of the glass be coated in a high vacuum with a grid made from a highly reflective metal--silver or aluminum--before it is bound to the modules.

Such a mirror mosaic is created by vacuum plating aluminum or silver through masks, thanks to which the configuration of the grid strips reiterates the arrangement of power distribution contacts and the intercontact gaps in the parallel modules. Because of the reflective grid on the back side of the glass, those spots occupied by the contacts reflect 84 percent of the solar radiation (in the case of aluminum) or 92-94 percent (in the case of silver). The absorptivity of those spots occupied by the contacts decreases because of this reflective grid from 0.75 to 0.16 or even 0.06-0.08, while the hemispheric emittance ε remains high, equal to 0.86, for both the silicon photoelectric transducers and the surface of the contacts. This is due also to the outer glass coating. The equilibrium temperature at those places occupied by the contacts drops, and the heat overflow from the heated semiconductor surface to the cooled contact spots leads to a reduction in the average equilibrium temperature of solar batteries.

For the solar batteries on the automatic interplanetary station "Venera-9," parallel modules made from silicon photoelectric cells are utilized which are transparent in the solar spectrum's infrared range. Heat-reflective coatings of vacuum-plated aluminum are also used on 10-12 percent of the internal surface of the protective glass on the parallel module. Protective radiation-resistant glass of 170 and 300 μm thicknesses was used in the modules. Also, the advantage of using one over-all coverglass for several photoelectric cells (a module consists of 4 to 6 photoelectric cells, each about 5 cm^2 in surface) is the improvement in radiation protection reliability.

Calculations have shown that the equilibrium temperature of such solar batteries should be 30-35°C lower along the entire Earth-Venus flight path in comparison with solar batteries of the usual design.

Temperature and Electrophysical Characteristics of High-Efficiency Photoelectric Cells Exposed to Elevated Temperatures. In accordance with the theory of photoelectric transducers with a p-n junction, developed in works [7-9], there exists a broad class of semiconductor compounds that have an advantage over silicon in the maximum feasible efficiency as well as in a number of operational characteristics. To this group of semiconductors belong the intermetallic compounds of the A_3B_5 system--gallium arsenide, indium phosphide, gallium phosphide as well as various combinations of these compounds. The most promising material from this group from the point of view of the production level and the results achieved is gallium arsenide (GaAs).

The temperature characteristics of these types of photoelectric transducers make it possible to obtain high specific characteristics. The difference in the dependence of the absorptivity upon the wavelength in comparison with silicon leads to yet another important feature of gallium arsenide photoelectric transducers--the contribution of the base toward the over-all collector efficiency is considerably less than the contribution of the diffusion region for the most probable parameters of the source material and the p-n junction. This means that the losses due to radiation transmission without absorption in gallium arsenide are considerably less. Thus, the same collector efficiencies and, consequently, the same over-all efficiencies can be obtained for gallium arsenide photelectric transducers with considerably thinner base layers. Because of this, one can obtain at least the same specific characteristics for photoelectric transducers made from silicon and gallium arsenide at room temperature, despite the doubled specific weight of gallium arsenide.

The temperature characteristics of the power parameters of the photocurrent, the photoelectromotive force and the efficiency of gallium arsenide photoelectric transducers have been studied in the +20 to +200°C temperature range. The results obtained for the efficiency are cited in fig. 1 (curves 1a, b). For comparison, the temperature dependence of the efficiency of silicon photoelectric transducers is also shown (curve 2, according to the data in work [10]). The indices a and b apply to samples that have a different magnitude of series resistance. From fig. 2 it is apparent that gallium arsenide-based photoelectric transducers have approximately one half the temperature gradient of efficiency in comparison with silicon

(-0.025%/°C for gallium arsenide). This difference is explained by the lesser dependence of the load current on the temperature in the interval studied and the greater initial values of the photoelectromotive force of the photoelectric transducers based on gallium arsenide.

An analysis has shown [11] that the attainment of minimum values for the inverse dark current of the p-n junction is decisive in obtaining temperature-stable solar cells. For gallium arsenide photoelectric transducers a value of 10^{-9} to 10^{-10} A/cm² for the inverse dark current is characteristic, while at the same time the values for this parameter for silicon photoelectric transducers lie in the 10^{-6} to 10^{-7} A/cm² interval.

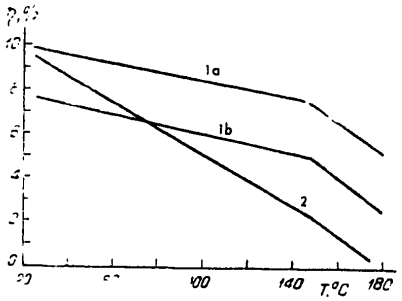

Fig. 1

Temperature dependence of gallium arsenide (curves 1a, b) and silicon (curve 2) photoelectric transducers.

The increase in the photocurrent when the light flux increases leads to a noticeable reduction in the optimum output temperature gradients of semiconductor photoelectric transducers. This condition must be taken into account when designing solar batteries for interplanetary solar stations directed toward the Sun.

It is apparent from fig. 1 that for the same initial efficiencies (at conditions of room temperature), gallium arsenide photoelectric transducers begin to surpass silicon photoelectric transducers by more than a factor of two at temperatures of 130 to 140°C, temperatures which were expected according to calculated data for the solar batteries on "Lunokhod."

Operating Conditions and Operational Characteristics of the Solar Batteries on "Lunokhod-I" and "Lunokhod-II." Semiconductor solar batteries for "Lunokhod-I" and "Lunokhod-II," made from gallium arsenide-based photoelectric transducers, are located on the inside of the lunar vehicle's roof, which, in its closed position, rests on the upper part of the body. In the operating position, the solar battery panel can be inclined at various angles, which makes possible the optimum utilization of the Sun's energy when its elevation over the lunar horizon varies.

In fig. 2 is represented the variation in the parameters of the "Lunokhod-II's" solar batteries over the course of the second and fourth lunar days. The operational temperature conditions are given as well. The slight increase in the current from the solar batteries at the beginning and end of the lunar day is explained by the effect of the cooling radiator in "Lunokhod's" thermoregulating system when the Sun is at low angles over the lunar horizon.

In fig. 3 the variation in the current from "Lunokhod-I's" solar batteries is shown. When the Sun's elevation over the lunar horizon is greater than 34°, the solar battery in the transport position (angle $\varphi=0$) makes it possible to obtain a current from the solar battery of not less than 4A, which insures the "Lunokhod's" operational routine when it is in motion.

The solar battery on "Lunokhod-I," the vehicle which was delivered to the Moon's surface on 17 November, 1970, functioned successfully over the course of 10 lunar days up through 4 October, 1971. In 10.5 months the degradation of the solar battery's working current amounted to about 6 percent. The solar batteries on "Lunokhod-II," delivered to the Moon's surface on 16 January, 1973, are based on gallium arsenide photoelectric transducers. They operated successfully for the entire period of the planned program of five lunar days without degradation of their electrophysical characteristics.

Experimental Investigations Into Certain Characteristics of the Solar Batteries on the Automatic Interplanetary Stations (AMS's) "Venera-9" and "Venera-10." The solar batteries on AMS's "Venera-9" and "Venera-10" consist of two rectangular panels of approximately 4 m^2 in surface area at each station. The panels are oriented toward the Sun along with the automatic interplanetary station itself.

The plane modules of the silicon photoelectric transducers, transparent in the IR-region of the solar spectrum when used in combination with the mirror mosaic over the current pick-off contacts, are fixed to the supporting surface of the panels.

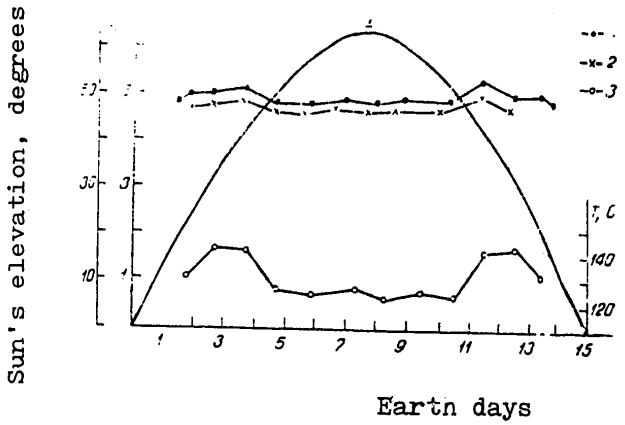

Fig. 2

Variations in the parameters of the solar batteries on the "Lunokhod-II"

1,2 - Solar battery current variation on "Lunokhod-II" during the course of the second and fourth lunar days;

3 - Solar battery temperature variation on "Lunokhod-II" during the second lunar day;

I - Variation in the Sun's elevation during the second lunar day, 8-22 February, 1973.

The panels have low thermal conductivity but, like the photoelectric transducers, they are transparent in the IR-region of the solar spectrum. The space factor of the panels with solar battery modules is 0.91.

In fig. 4 is shown the variation in the irradiance on the panel of solar batteries on the "Venera-9" and "Venera-10" automatic interplanetary stations. The abrupt variation in the currents from the solar batteries is explained by the switching on and off of portions of the solar battery as provided for in the station's program.

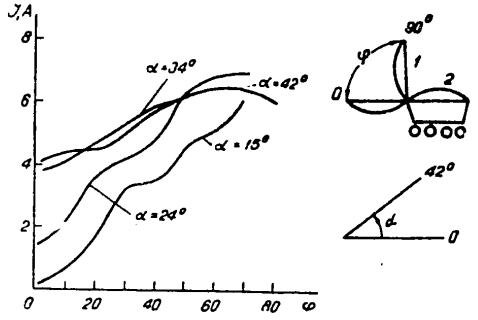

Fig. 3

Solar battery current variation on "Lunokhod-I" when the panel was used to scan the Sun's elevation at various positions. When the normal to the solar battery was oriented toward the Sun along an azimuth having an error no greater than ±4°, α is the Sun's elevation over the lunar horizon; φ is the inclination of the solar battery relative to the horizon. 1 - Solar batteries; 2 - Cooling radiator of the thermoregulating system.

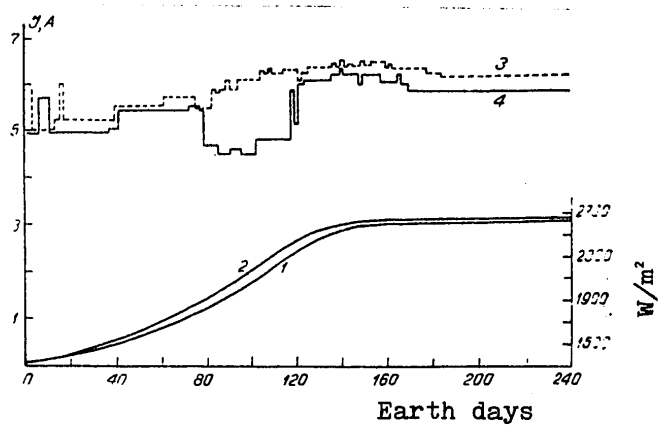

Fig. 4

Variation in the irradiance of the solar battery panel on the "Venera-9" (1) and "Venera-10" (2) automatic interplanetary stations along the stations' flight path. Variation in the solar battery operating currents on the

"Venera-9" (3) and "Venera-10" (4) automatic interplanetary stations along the Earth-Venus flight paths (segment "a") and along the orbits of artificial satellites of Venus (segment "b").

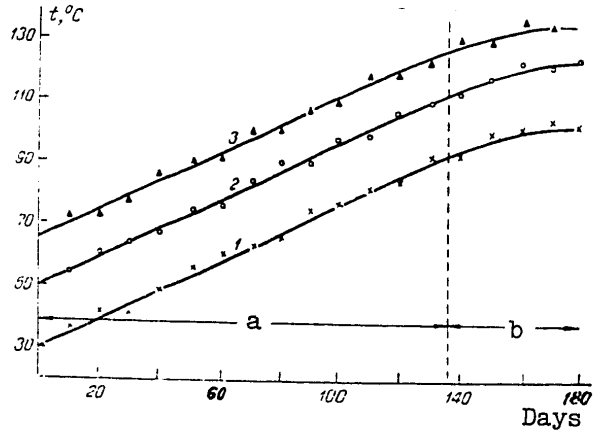

Fig. 5

Variation in operating temperatures of the photoelectric transducers in the solar batteries of "Venera-9" and "Venera-10" (1) and of silicon photoelectric transducers of the usual design that are not transparent in the IR-region of the solar spectrum, with a mirror mosaic over the contacts (2) and without it (3) along the Earth-Venus flight paths (segment "a") and along orbits of artificial satellites of Venus (segment "b").

In fig. 5 are represented the variations in the operating temperatures of the photoelectric transducers of the solar batteries on "Venera-9" and "Venera-10," which had practically the same temperature variation along the entire flight path (a). Photoelectric transducers of the usual design were mounted alongside the panels of solar batteries on "Venera-9" and "Venera'10" in the form of sensors on frame-extension brackets.

The utilization of the mirror mosaic leads to a 15°C decrease in the operational equilibrium temperature of photoelectric transducers of the usual design, while the simultaneous application of the mirror mosaic and photoelectric transducers that are transparent in the IR-region of the solar spectrum leads

to a 33-35°C reduction in the operational equilibrium temperature along the entire flight path of the "Venera-9" and "Venera-10" automatic interplanetary stations.

As a result of the research that has been carried out, high efficiency silicon- and gallium arsenide-based solar batteries have been developed which successfully insure the operation of the Soviet "Venera-9" and "Venera-10" automatic stations and the "Lunokhod" vehicles. The results of development and research have been confirmed by successful testing of the solar batteries under operating conditions.

BIBLIOGRAPHY

1. Koltun, M. M. and Landsman, A. P. "Preobrazovateli solnechnoy energii na poluprovodnikakh" [Semiconductor Solar Energy Transducers], Moscow, 1968.

2. Koltun, M. M. and Landsman, A. P. KOSMICHESKIYE ISSLEDOVANIYA, No 2, 1964.

3. Koltun, M. M. and Landsman, A. P. OPTIKA I SPEKTROSKOPIYA, No 26, 1969.

4. Thelen, A. Conf. paper 1296-60, ARS Conf., Santa Monica, California, 27 Sep 60.

5. SPACEFLIGHT, No 9, 1967.

6. Koltun, M. M. GELIOTEKHNIKA, No 6, 1970.

7. Loferski, I. I. J. APPL. PHYS., Vol 27, No 7, 1956.

8. Loferski, I. I. ACTA ELECTRONICA, Vol 5, No 3, 1961.

9. Toss, T. S. SOLID STATE ELECTRONICS, Vol 12, No 4, 1961.

10. Zaytseva, A. K. and Gliberman, A. Ya. "Kremniyevyye solnechnyye batarei" [Silicon Solar Batteries], Moscow, 1961.

11. Kagan, M. B., Landsman, A. P. and Lyubashevskaya, T. L. KOSMICHESKIYE ISSLEDOVANIYA, Vol 9, No 4, 1971.

[8144/1143-9512]

9512
CSO: 8144/1143

HIGH-ENERGY DEVICES, OPTICS AND PHOTOGRAPHY

UDC 536.3

ANGULAR COEFFICIENTS FOR A PARTLY SHIELDED CYLINDRICAL SURFACE

Minsk INZHENERNO-FIZICHESKIY ZHURNAL in Russian Vol 37, No 3, Sep 79
pp 522-523

[Annotation of deposited article by V. A. Arkhipov, registration number 1377-79 Dep.]

[Text] A method of numerical integration is used to determine the angular coefficients of radiation between the surfaces of a disk and an infinite cylinder separated by a screen that is oriented parallel to the disk and has a diaphragm coaxial with the disk. The normal to the center of the disk passes through the axis of the cylinder and is perpendicular to this axis. A configuration of this type is of interest in particular in the design of opto-electronic equipment for laser diagnosis of axisymmetric plasma jets. The average angular coefficient was calculated from the general formula for $\phi_{1,2}$ written for application to the given geometry:

$$\varphi_{1,2}=\frac{4R}{(\pi r_1)^2}\int_0^{z_k} dz \int_0^{\xi_k} (L-R\cos\xi)\,d\xi \int_0^{r_1} r\,dr \times$$

$$\times \int_0^{2\pi} \frac{(r\sin\xi\sin\psi+L\cos\xi-R)\,d\psi}{(R^2+L^2+z^2+r^2-2RL\cos\xi-2r\cos\psi-2rR\sin\xi\sin\psi)^2}.$$

For the variables of the limits of integration $z_k(r,\psi,\xi)$, $\xi_k(r,\psi)$ that determine the field of view, we get the analytical expressions

$$z_k=r\cos\psi+\frac{L-R\cos\xi}{l}\left(\sqrt{r_2^2-\left(r\sin\psi+\frac{l(R\sin\xi-r\sin\psi)}{L-R\cos\xi}\right)^2}-r\cos\psi\right),$$

$$\xi_k=\arcsin\frac{Lr_2-(L-l)r\sin\psi}{R\sqrt{l^2+(r_2-r\sin\psi)^2}}-\operatorname{arctg}\frac{r_2-r\sin\psi}{l}.$$

On the basis of an algorithm derived in this paper, numerical calculations are done and curves are plotted for the average angular coefficients, and for local angular coefficients (with contraction of the disk to an

element of area) for different values of the geometric parameters of the given radiating system.

Notation

l--distance between disk and screen; L--distance between disk and axis of cylinder; r, ψ--cylindrical coordinates of a point on the surface of the disk; r_1--radius of the disk; r_2--radius of the diaphragm; R--radius of the cylinder; z, ξ--cylindrical coordinates of a point on the surface of the cylinder.

6610
CSO: 1861

FLUID MECHANICS

UDC 532.526-597.31

EXPERIMENTAL STUDY OF THE INFLUENCE THAT PLIABLE SURFACES HAVE ON THE INTEGRAL CHARACTERISTICS OF A BOUNDARY LAYER

Minsk INZHENERNO-FIZICHESKIY ZHURNAL in Russian Vol 37, No 3, Sep 79 p 518

[Annotation of deposited article by V. I. Korobov, registration number 1368-79 Dep.]

[Text] Previous research has been done on the interaction between pliable boundaries and an oncoming flow. Most of these studies have been done in air and on surfaces of diaphragm type. Based on hydrobionic studies, there is an opinion that elastic surfaces such as animal hides play an active functional part in the hydrodynamics of aquatic animals.

The paper gives the results of an experimental study of the hydrodynamic friction of pliable surfaces of monolithic type, with consideration of the morphofunctional structure of the outer hides of aquatic animals. The experiments were done in a hydrochute, using an insert placed on a strain-gage bracket in the lower wall of the working section.

The principal results of the work can be formulated as follows.

Pliable surfaces may have an appreciable effect on the integral characteristics of a boundary layer; a pliable surface with constant mechanical characteristics has its own comparatively narrow range with respect to Reynolds numbers with an extremum of effective action on a boundary layer with position and extent that depend on a number of surface parameters.

6610
CSO: 1861

UDC 531.38

CONCERNING THE EFFECT OF WHITE NOISE ON THE PROCESS OF INERTIAL SEPARATION

Minsk INZHENERNO-FIZICHESKIY ZHURNAL in Russian Vol 37, No 3, Sep 79 pp 519-520

[Annotation of deposited article by Ye. A. Yeseyev, registration number 1375-79 Dep.]

[Text] The stochastic differential equation

$$\frac{dr}{dt} = \tau\left(1 - \frac{\rho}{\rho_1}\right)\frac{v_\varphi^2}{r} + g\xi(t) \qquad (1)$$

is valid for steady-state turbulent motion of a swirling dispersed system in which it is assumed that the trajectories of all particles of the carrier fluid are arcs of concentric circles on the average, and the motion of the suspended matter (Stokes fractions) relative to the dispersion medium is quasi-steady. Ref. 2 tells us that the equation

$$\frac{\varepsilon g^2}{2}\frac{d^2f(r_0)}{dr_0} + \tau\left(1 - \frac{\rho}{\rho_1}\right)\frac{v_\varphi^2}{r_0}\frac{df(r_0)}{dr_0} = -1. \qquad (2)$$

corresponds to (1).

Taking $v_\phi = \text{const}\, r^\gamma$, and approximating some tangential velocity profile of the carrier fluid by $\gamma = 0.5$, we write (1) in dimensionless form

$$\alpha\frac{d^2\bar{f}(\bar{r}_0)}{d\bar{r}_0^2} + \beta\frac{d\bar{f}(\bar{r}_0)}{d\bar{r}_0} = -1, \qquad (3)$$

where α, β are the dimensionless coefficients of diffusion and drift respectively.

If equation (2) is considered in conjunction with the boundary conditions

$$\frac{d\bar{f}(\bar{R}_1)}{d\bar{r}_0} = 0, \quad \bar{f}(\bar{R}_2) + \lambda\frac{d\bar{f}(\bar{R}_2)}{d\bar{r}_0} = 0, \qquad (4)$$

it has the solution

$$f(\bar{r}_0) = \frac{\bar{R}_2 - \bar{r}_0}{\beta} - \frac{\alpha}{\beta^2}\left\{\exp\left[-\frac{\beta}{\alpha}(\bar{r}_0 - \bar{R}_1)\right] - \right.$$
$$\left. - \exp\left[-\frac{\beta}{\alpha}(\bar{R}_2 - \bar{R}_1)\right]\right\} + \frac{\lambda}{\beta}\left\{1 - \exp\left[\frac{\beta}{\alpha}(\bar{R}_2 - \bar{R}_1)\right]\right\}. \quad (5)$$

Here $\bar{R}_1$, $\bar{R}_2$ are the inner and outer boundaries of the separation zone, λ is a parameter that characterizes the intensity of burbling of the particles of some fraction from boundary $\bar{R}_2$. It is apparent from (5) that the first term is always positive, the second is always negative, and the third is determined by the parameter λ.

Verification of the feasibility of result (5) with some other empirical values of v_ϕ, specifically when $\gamma = 1$, -1, based on numerical integration of the direct Fokker-Planck-Kolmogorov equation for probability density $w(\bar{r}, \bar{t})$ of process $\bar{r}(\bar{t})$with conditions on $\bar{R}_1$, $\bar{R}_2$ analogous to (4) showed complete agreement between the data of the calculation and (5). As the coefficient α increases, there is an increase in the calculated fraction efficiencies for the corresponding values of $\bar{t}$ of the interval of process duration, and this trend is not at all disrupted by the form of v_ϕ.

Notation

r, ϕ--polar coordinates; t--time; v_ϕ--tangential component of the velocity field of the dispersion medium; τ--relaxation time of a separated particle; ρ, ρ_1--physical densities of medium and particle respectively; g--parameter that characterizes the specific dispersed system; ξ, ε--white noise and its intensity respectively; f--average time for a particle to reach the boundary; r_0--initial distribution of polar radius; $\bar{r}_0 = \frac{2r_0}{R_1 + R_2}$, $\bar{f}$, etc.--dimensionless characteristics of the corresponding quantities.

REFERENCES

1. N. A. Fuks "Mekhanika aerozoley" [Mechanics of Aerosols], Moscow, Academy of Sciences USSR, 1955.

2. Yu. V. Prokhorov, Yu. A. Rozanov, "Spravochnaya matematicheskaya biblioteka. Teoriya veroyatnostey. Osnovnyye ponyatiya. Predel'nyye teoremy. Sluchaynyye protsessy" [Mathematics Reference Library. Probability Theory. Basic Concepts. Limit Theorems. Random Processes], Moscow, Nauka, 1967.

3. E. Rammler, R. Beuerfeind, STAUB, 134, No 5, 1959.

[64-6610]
6610

CSO: 1861

UDC 536.24

RADIATIVE HEAT EXCHANGE IN A SYSTEM OF TWO COAXIAL CYLINDERS WITH AN INTERMEDIATE PERFORATED CYLINDER

Minsk INZHENERNO-FIZICHESKIY ZHURNAL in Russian Vol 37, No 3, Sep 79 p 522

[Annotation of deposited article by A. V. Rumyantsev, O. N. Bryukhanov and V. R. Bazilevich, registration number 1374-79 Dep.]

[Text] The resultant radiation energy fluxes between the components of a system of three infinitely long coaxial cylinders with perforations in the middle cylinder are found in the diffuse approximation from predetermined temperatures and geometric-optics properties. The problem is solved by a generalized zonal method. For this purpose, expressions were found for the average angular coefficients of radiation:

$$\varphi_{14} = \beta, \quad \varphi_{12} = 1 - \beta, \quad \varphi_{22} = (1 - \zeta_{12})(1 - \beta),$$
$$\varphi_{21} = \zeta_{12}, \quad \varphi_{24} = \beta(1 - \zeta_{12}), \quad \varphi_{42} = \zeta_{24}(1 - \beta)\varphi_{24},$$
$$\varphi_{41} = \beta\zeta_{14}, \quad \varphi_{43} = (1 - \beta)\zeta_{34}, \quad \varphi_{44} = 1 - \zeta_{24}[1 - \beta^2(1 - \zeta_{12})].$$

Here $\zeta_{ik} = D_i/D_k$ is the ratio of diameters of the cylindrical surfaces, β is the degree of perforation of surface F_2. Quantities relating to convex surfaces have subscripts 1 and 3, while those referring to concave surfaces have subscripts 2 and 4.

Numerical analysis of the resultant computational relations shows nonlinear dependence of the resultant energy fluxes radiated by surfaces F_2 and F_4 as a function of β. The energy flux from surface F_1 increases monotonically with increasing β, which is attributed to the reduction in screening action of the perforated cylinder. The energy flux radiated by surface F_3 falls linearly with increasing β due to the reduction in its area. The energy fluxes radiated by surfaces F_2 and F_4 are nonlinear functions of the variable β.

The function that describes the resultant flux from surface F_2 to surface F_4 has a maximum that shifts toward smaller β as the values of ε decrease. The peculiarities of radiation of this surface are due to the following

factors that differ in their effect on the nature of radiation of this surface: 1) the perforation effect (cavity effect); 2) change in the radiation flux incident on the exposed surface with a change in the area of the perforations; 3) change in the area of the radiating surface with a change in β. These factors are responsible both for the nonlinearity of the function and for the maximum in this function.

The intermediate perforated cylinder can be treated as a perforated screen between the unperforated cylinders. A comparison of the energy fluxes incident on surface F_4 with a perforated or an unperforated screen in the system as plotted at identical temperatures shows that this ratio is greater than unity for any values of ε and β. The difference between fluxes increases with a reduction in ε, which can be attributed to the perforation effect that has a considerable influence on the type of radiation of surface F_2.

The resultant computational formulas can also be used to find the energy radiated by a coaxial system made up of an inner unperforated cylinder and an outer perforated cylinder.

[64-6610]

6610
CSO: 1861

UDC 536.3

HEAT EXCHANGE OF A TWO-LAYER PLATE WITH A MOVING RADIATING AND SCATTERING MEDIUM

Minsk INZHENERNO-FIZICHESKIY ZHURNAL in Russian Vol 37, No 3, Sep 79 pp 523-524

[Annotation of deposited article by F. N. Lisin and I. F. Guletskaya, registration number 1380-79 Dep.]

[Text] A gray radiating, absorbing and scattering medium moves in a slot channel with gray walls. The lower wall is a two-layer plate with given thickness and coefficient of thermal conductivity. The velocity profile is parabolic. On the lower boundary of the two-layer plate the heat flux is given as a function of the coordinate x. The temperature of the upper wall T_{CT} is constant. The problem is written in dimensionless form as follows:

equation of energy for the medium:

$$\mathrm{Pe}\frac{u(\eta)}{\bar{u}}\frac{\partial\theta}{\partial\bar{x}}=\frac{\partial^2\theta}{\partial\eta^2}-\frac{\mathrm{Pe}}{\mathrm{Bo}}\operatorname{div}\bar{q}; \tag{1}$$

equation of heat transfer in the layers of the plate

$$\frac{\partial^2\theta_l}{\partial\bar{x}^2}+\frac{\partial^2\theta_l}{\partial\eta^2}=0,\ l=1,\ 2\text{ are the numbers of the layers} \tag{2}$$

with boundary conditions

$$\theta=1 \quad \text{at}\ \bar{x}=0;\ \ \theta=\theta_{CT} \ \text{at}\ \bar{x}>0;\ \ \eta=1;$$

$$\frac{\partial\theta}{\partial\eta}-\frac{\mathrm{Pe}}{\mathrm{Bo}}\bar{q}_{CT}=k_1\frac{\partial\theta_1}{\partial\eta}\ \text{at}\ \eta=0;$$

$$\theta(\bar{x},\ 0)=\theta_1(\bar{x},\ 0);\quad \frac{\partial\theta_1}{\partial\bar{x}}=\frac{\partial\theta_2}{\partial\bar{x}}=0\ \text{at}\ \bar{x}=0,\ \bar{x}=L,$$

$$k_2\frac{\partial\theta_1}{\partial\eta}=\frac{\partial\theta_2}{\partial\eta},\quad \theta_1(\bar{x},\ \eta)=\theta_2(\bar{x},\ \eta)\ \text{at}\ \eta=-\bar{S}_1,$$

$$\frac{\partial\theta_2}{\partial\eta}=\bar{q}_2(\bar{x})\ \text{at}\ \eta=-\bar{S}_2.$$

where $\eta = y/b$; $\bar{x} = x/b$; $\bar{\theta} = T/T_0$; $k_1 = \lambda_1/\lambda$; $k_2 = \lambda_1/\lambda_2$; $\bar{S}_1 = S_1/b$; $\bar{S}_2 = S_2/b$; $\bar{q}' = q'(\bar{x})/\sigma_0 T_0^4$.

The divergence of radiant flux is found from solution of the transport equation in the P_1 approximation of the method of spherical harmonics, and contains the average scattering cosine. The influence that optical thickness has on the Nusselt numbers of radiant and convective heat fluxes to the plate and to the upper wall is analyzed on the basis of the numerical solution. The amount of heat transferred by radiation to the walls with changing $\tau_0(1 - \gamma)$ passes through a maximum in the vicinity of 1.1-1.2 (τ_0 is the optical thickness, γ is the ratio of the scattering coefficient to the attenuation factor). Calculations are used to analyze the influence that the ratio of the coefficients of thermal conductivity of the plates $k_2 = \lambda_1/\lambda_2$ has on heat exchange. As k_2 increases, there is a rise in temperature on the boundary $\eta = 0$, which has an effect on cooling of the medium in the channel. The higher the k_2, the higher will be the corresponding curves for the Nusselt numbers of the radiant heat flux as dependent on channel length.

6610
CSO: 1861

UDC 536.21

DYNAMIC TEMPERATURE FIELDS IN HOLLOW HOMOGENEOUS SPHERICAL BODIES

Minsk INZHENERNO-FIZICHESKIY ZHURNAL in Russian Vol 37, No 3, Sep 79 pp 527-529

[Annotation of deposited article by V. V. Semenyuk and M. P. Lenyuk, registration number 1369-79 Dep.]

[Text] Dynamic problems of the classical theory of linear thermoelasticity require knowledge of the true temperature field accompanying high-intensity unsteady processes. In such processes the temperature field in an isotropic homogeneous hollow spherical body $D=\{(r,\theta,\phi), R_1 \leqslant r \leqslant R_2,\ 0 \leqslant \theta \leqslant \pi,\ 0 \leqslant \phi \leqslant 2\pi\}$ is described by a scalar quantity T that is the solution of a generalized (hyperbolic) heat conduction equation [Ref. 1]

$$L[T] = b_0^2 \frac{\partial^2 T}{\partial t^2} + b_1^2 \frac{\partial T}{\partial t} - a^2 \left(\frac{\partial^2 T}{\partial r^2} + \frac{2}{r} \frac{\partial T}{\partial r} + \right.$$

$$\left. + \frac{1}{r^2} \left\{ \frac{\partial}{\partial \mu} \left[(1-\mu^2) \frac{\partial T}{\partial \mu} \right] + \frac{1}{1-\mu^2} \frac{\partial^2 T}{\partial \varphi^2} \right\} \right) = f_1(t, r, \mu, \varphi),\ \mu = \cos\theta \qquad (1)$$

with respect to initial and boundary conditions

$$T|_{t=0} = f_2(r, \mu, \varphi),\ \left.\frac{\partial T}{\partial t}\right|_{t=0} = f_3(r, \mu, \varphi), \qquad (2)$$

$$\left(h_{j1} \frac{\partial}{\partial r} + h_{j2} \frac{\partial}{\partial t} + h_{j3} \right) T|_{r=R_j} = (-1)^{j+1} \psi_j(t, \mu, \varphi),\ j = 1, 2 \qquad (3)$$

and conditions of single-valuedness relative to (ϕ,θ).

The solution of problem (1)-(3) is constructed by means of the principal solutions (fundamental functions) of the problem, and takes the form

$$T = \int_0^t d\tau \int_0^{2\pi} d\alpha \int_{-1}^{+1} d\eta \int_{R_1}^{R_2} E(t-\tau;\ r,\ \rho;\ \mu,\ \eta;\ \varphi,\ \alpha)\,\rho^2 f_1(\tau,\ \rho,\ \eta,\ \alpha)\,d\rho +$$

$$+ \int_0^t d\tau \int_0^{2\pi} d\alpha \int_{-1}^{+1} [W_-(t-\tau;\ r,\ \mu,\ \eta;\ \varphi,\ \alpha)\,\psi_1(\tau,\ \eta,\ \alpha) + W_+(t-\tau;\ r,\ \mu,\ \eta;\ \varphi,\ \alpha) \times$$

$$\times \psi_2(\tau,\ \eta,\ \alpha)]\,d\eta + \int_0^{2\pi} d\alpha \int_{-1}^{+1} d\eta \int_{R_1}^{R_2} K(t,\ r,\ \rho;\ \mu,\ \eta;\ \varphi,\ \alpha)\left[f_2(\rho,\ \eta,\ \alpha) + \right. \qquad (4)$$

$$\left. + \frac{b_1^2}{b_0^2} f_3(\rho,\ \eta,\ \alpha)\right]\rho^2 d\rho + \frac{\partial}{\partial t}\int_0^{2\pi} d\alpha \int_{-1}^{+1} d\eta \int_{R_1}^{R_2} K(t,\ r,\ \rho;\ \mu,\ \eta;\ \varphi,\ \alpha)\,f_3(\rho,\ \eta,\ \alpha)\,\rho^2 d\rho.$$

An important part in construction of the fundamental functions E, K, $W_{\pm}$ of problem (1)-(3) is played by the finite direct Λ_{mn} and inverse Λ_{nm}^{-1} integral Legrange-Fourier transforms

$$\Lambda_{nm}[f(\varphi,\ \mu)] = \int_{-1}^{+1}\int_0^{2\pi} f(\varphi,\ \mu)\,e^{im\varphi}P_n^m(\mu)\,d\varphi d\mu = f_{nm}, \qquad (5)$$

$$\Lambda_{nm}^{-1}[f_{nm}] = \frac{1}{\pi}\,\mathrm{Re}\sum_{m=0}^{\infty}\sum_{n=0}^{\infty}\varepsilon_m \frac{f_{nm}e^{-im\varphi}P_n^m(\mu)}{\|P_n^m(\mu)\|^2} = f(\varphi,\ \mu), \qquad (6)$$

where $P_n^m(\mu)$ is an associated Legendre polynomial of the first kind [Ref. 2];

$$\varepsilon_m = \begin{cases} \frac{1}{2}, & m = 0 \\ 1, & m > 1 \end{cases}, \quad \|P_n^m(\mu)\|^2 = \frac{2(n+m)!}{(2n+1)(n-m)!} \text{ is the square of the norm}$$

Operator Λ_{nm} in combination with the integral Laplace operator [Ref. 3] reduces the three-dimensional problem to a one-dimensional problem.

Parameters h_{ij} (i, j = 1, 3) enable us to single out solutions of problem (1)-(3) from formula (4) for any combination of the first three kinds of boundary conditions assigned on any of the surfaces $r = R_j$ (j = 1, 2); and the non-negative arbitrary parameters b_0, b_1 can be used to get purely wave-type temperature fields ($b_1 \to 0$) as well as ordinary (parabolic) temperature fields ($b_1 = 1$, $b_0 \to 0$).

As an example, the authors consider the case where there is no heat source in sphere D ($f_1 = 0$), the initial temperature of the sphere is zero ($f_2 = f_3 = 0$), boundary $r = R_1$ is held at zero temperature, and the boundary $r = R_2$ of the sphere is heated by the law $\psi_2 = t_0 S_+(t)(1-\mu)^{-\frac{1}{2}}$, $S_+(t)$ is an asymmetric unit function.

REFERENCES

1. A. V. Lykov, "Teoriya teploprovodnosti" [Theory of Heat Conduction], Vysshaya shkola, 1967, p 600.

2. Ye. B. Gobson, "Teoriya sfericheskikh i ellipsoidal'nykh funktsiy" [Theory of Spherical and Ellipsoidal Functions], Moscow, IL, 1952, p 476.

3. M. A. Lavrent'yev, B. V. Shabat, "Metody teorii funktsiy kompleksnogo peremennogo" [Methods of the Theory of Functions of a Complex Variable], Moscow, 1973, p 736.

6610
CSO: 1861

UDC 532.517.4

CALCULATION OF SURFACE FRICTION OF THE INITIAL SECTIONS OF PIPES IN A TURBULENT BOUNDARY LAYER WITH SWIRLING OF THE FLOW AT THE INLET

Minsk INZHENERNO-FIZICHESKIY ZHURNAL in Russian Vol 37, No 3, Sep 79 pp 532-533

[Annotation of deposited article by V. M. Sobin, registration number 709-79 Dep.]

[Text] An approximate method is given for calculating surface friction in a turbulent boundary layer of incompressible fluid with swirling of the flow at the inlet.

The problem is solved by an integral method [Ref. 1] that is conservative with respect to the exact velocity profile in the case of correct modeling of the region near the wall. The equations of motion in the boundary layer in the cylindrical coordinate system with corresponding boundary conditions are reduced to a system of two nonlinear ordinary differential equations of first order relative to the parameters of surface friction λ and s. For the axial velocity component in the boundary layer the author uses the universal logarithmic profile $u^+ = 2.5 \ln y^+ + 5.5$, and for tangential velocity -- $w^+ = u^+ s$. In doing so, s is taken as a function of x alone. An estimate of the magnitude of the terms of the resultant equations enabled simplification. As a result, the equations for λ are given as

$$\delta^+ (\lambda^2 - 5\lambda + 12{,}5) \frac{d\lambda}{dx} + \frac{\bar{u}_0}{u_0} 5\delta^+\lambda (\lambda - 2{,}5) = \mathrm{Re}\, \bar{u}_0. \qquad (1)$$

By using the approximations

$$\delta^+ (\lambda^2 - 5\lambda + 12{,}5) = 1{,}9 \exp(0{,}545\lambda),$$
$$5\delta^+\lambda (\lambda - 2{,}5) = 11{,}1 \exp(0{,}545\lambda) \qquad (2)$$

equation (1) can be solved analytically.

It has been shown that $\bar{u}_0 = \mathrm{const}$ for many practical cases. When this condition is considered, the equation for s takes the form

$$\frac{ds}{d\bar{x}}+\left[\frac{\mathrm{Re}\,\bar{u}_0}{\delta^+\lambda\,(\lambda^2-5\lambda+12{,}5)}-\frac{1}{\lambda}\,\frac{d\lambda}{d\bar{x}}\right]s=0 \qquad (3)$$

and is readily integrated by using the first approximation (2).

The following explicit relations are finally obtained for c_f and s:

$$c_f=\frac{0{,}594}{\ln^2\left(\frac{z_0}{\bar{x}_0}\bar{x}\right)} \qquad (4)$$

$$s=s_0\frac{c_f}{c_{f_0}} \qquad (5)$$

in which the constants are corrected with consideration of experimental data.

It is interesting to note that formula (4) also gives a good description of the total coefficient of surface friction, and (5) predicts self-similarity of the angles of twist of the flow with a high degree of accuracy with respect to Reynolds number.

Notation

$\bar{x}=x/d$ -- dimensionless longitudinal coordinate; u_0 -- the value of u on the boundary layer; s -- tangent of angle of twist of the flow relative to the axis of the tube in direct proximity to the wall; τ_{10} -- axial component of shearing stress at the wall; x_0, s_0, λ_0 -- the values of x, s and λ in the initial section; $u^+=u/u_*$; $y^+=yu_*/\nu$; $u_*=\sqrt{\tau_{10}/\rho}$; $c_f=2\tau_{10}/\rho u_0^2$; $\lambda=u_0/u_*=(2/c_f)^{1/2}$; $\bar{u}_0=u_0/u_{cp}$; $\delta^+=\exp\left(\frac{\lambda-5{,}5}{2{,}5}\right)$; $z_0=\exp(0{,}545\lambda_0)$; $\mathrm{Re}=u_{cp}d/\nu$.

REFERENCES

1. F. M. White, TRANS. ASME, SER. D, 91, N 3, 1969.

6610
CSO: 1861

UDC 534.14

CONCERNING THE PROBLEM OF THE ROLE OF CAVITATION IN THE ULTRASONIC CAPILLARY EFFECT

Minsk INZHENERNO-FIZICHESKIY ZHURNAL in Russian Vol 37, No 3, Sep 79 p 537

[Annotation of deposited article by V. G. Barantsev and V. N. Motorin, registration number 711-79 Dep.]

[Text] A series of experiments is done to study the effect of ultrasound on the capillary rise of liquids. Particular emphasis is given to the determination of the physical principles that lead to an increase in the capillary head under the action of ultrasound.

For this purpose, an experimental facility was set up including a measurement system with registration of the instantaneous rate of movement of the fluid through the capillary on motion picture film. The experiments were done under the following conditions: emitter power $N = 25$ W, frequency of oscillations $f = 41$ kHz, diameters of capillaries $d = 0.21$, 0.61, 1.16, 2.0 and 3.0 mm. Working fluids were water, ethyl alcohol, and transformer oil. The amplitude of sound pressure in the liquid was measured by a hydrophone. Data of experiments are given for $P_0 = 1.58$ atm.

The experimental results showed the behavior of the rate of rise of the liquid in the capillary as a function of time, capillary diameter, and type of liquid. An investigation was also made of the way that the distance from the emitter to the face of the capillary affects the rate of rise. The results of the experiments are given in the form of graphs of the function $h = f(\tau)$, where τ is the time interval during which the liquid level rises by a height h. Simultaneous measurements were made of the maximum height of rise of the liquid as a function of the diameter of the capillaries. For the capillary 3.0 mm in diameter, this height exceeded the equilibrium height of rise of the liquid without ultrasound by a factor of 105.4.

Cavitation in the liquid was observed visually, and also photographed by a microscope with camera adapter. In all experiments it was noted that

the rate of liquid rise reaches its maximum when the face of the capillary is set in the cavitation cloud or just above it. Results were stable with realization of this same condition.

The cavitation effect is observed only when the intensity of ultrasound exceeds the threshold value. When the amplitude of the sound wave falls below the threshold, the cavitation effects in the liquid stop, and the column of liquid falls to the equilibrium height of capillary rise without ultrasound.

The results of the experiments confirm the conclusion that acoustic cavitation in liquid is responsible for the ultrasonic capillary effect.

The authors offer a physical model which in their view explains the process of liquid rise in a capillary under the action of ultrasound, consisting in shearing off of part of the normal amplitude of the ultrasonic wave during the rarefaction phase due to the formation of ultrasonic cavitation in the liquid. It is suggested that acoustic cavitation in the liquid leads to the clipping of part of the amplitude of the ultrasonic wave during the phase of rarefaction. The level of cutoff is determined empirically by a coefficient (κ) that depends on the conditions of the experiment -- capillary diameter, kind of liquid and so on.

6610
CSO: 1861

UDC 539.377

GENERAL SOLUTION OF THE THERMOELASTIC PROBLEM FOR AN ASYMMETRICALLY HEATED SOLID CYLINDER

Minsk INZHENERNO-FIZICHESKIY ZHURNAL in Russian Vol 37, No 3, Sep 79 pp 537-538

[Annotation of deposited article by A. G. Sabel'nikov, K. I. Skorikov and A. N. Strigunov, registration number 1023-79 Dep.]

[Text] The authors consider an unbounded solid cylinder of radius R subjected to asymmetric heating in the peripheral direction.

The thermally stressed state of the cylinder is defined by the stress function $\Phi = \Phi(r,\phi,\tau)$ that is a general solution of the inhomogeneous biharmonic equation

$$\Delta(\Delta\Phi) = \frac{1+\mu}{1+\mu}\Delta\beta t. \qquad (1)$$

To find the components of the stress tensor σ_{ij} (i, j = r, ϕ, z) the temperature field $t = t(r,\phi,\tau)$ is represented as the sum of two terms:

$$t(r, \varphi, \tau) = t_1(r, \tau) + t_2(r, \varphi, \tau). \qquad (2)$$

Here $t_1(r,\tau)$ is the symmetric component of the temperature field, and $t_2(r,\phi,\tau)$ is the asymmetric component.

Then the stresses defined by (1) are the sum of two solutions of the problem of thermoelasticity, one of which corresponds to $t_1(r,\tau)$ and is found by conventional methods. The second solution, corresponding to $t_2(r,\phi,\tau)$, is found from the thermoelastic potential of displacements $\Phi = \Phi(r,\phi,\tau)$ satisfying the equation

$$\Delta\bar{\Phi} = \frac{1+\mu}{1-\mu}\beta t_2(r, \varphi, t), \qquad (3)$$

and from the general solution of equation (1) without the second member. The components of the stress tensor are represented in dimensionless

form. From the given general solutions, special cases can be obtained that correspond to symmetric heating of an unbounded solid cylinder and that agree completely with known solutions.

The authors consider an example of practical application of the derived solutions. This was done by using experimental data on heating of solid cylindrical workpieces by attacking jets in a convective velocity heating furnace.

Notation

r -- radial coordinate in meters; ϕ -- angular coordinate; τ -- time in seconds; μ -- Poisson's ratio; β -- coefficient of temperature expansion in 1/°C; $\Delta=\frac{\partial^2}{\partial r^2}+\frac{1}{r}\frac{\partial}{\partial r}+\frac{1}{r^2}\frac{\partial^2}{\partial\varphi^2}$ -- Laplace operator.

6610
CSO: 1861

END